

# Diffraction-Induced Stray Light in Infrared Microspectroscopy and Its Effect on Spatial Resolution

A. J. SOMMER\* and J. E. KATON

*Molecular Microspectroscopy Laboratory, Department of Chemistry, Miami University, Oxford, Ohio 45056*

Model experiments were conducted in an effort to quantitatively assess the extent of stray light, resulting from diffraction, in an FT-IR microscope system. The effects of stray light were studied under conditions employing different aperturing modes, aperture sizes, and wavelengths of light. Results and consequences of the findings are discussed with respect to the spatial resolution and quantitative integrity of the data obtainable in mapping analyses of multilayer polymer laminates.

Index Headings: Infrared microspectroscopy; Polymer laminates; Mapping analysis; Diffraction effects; Spatial resolution; Quantitative analysis.

## INTRODUCTION

Infrared microspectroscopy is widely employed for the analysis of individual layers in cross-sectioned multilayer polymer laminates. By optical isolation of the layer of interest with a remote aperture, it can easily be analyzed with minimal interference from neighboring layers provided that the thickness of the layer is on the order of 100 micrometers or larger. If the thickness of the layer is less than this dimension, the ability to obtain spectra without interference from neighboring layers becomes more difficult. This difficulty arises from diffraction effects associated with the various optical components of the microscope. As a result, the image of the infrared source and/or sample is redistributed to areas outside that defined by the aperture. Consequently, the spectrum of the single layer will be contaminated with spectral features from neighboring layers. The current trend in mapping analyses by infrared microspectroscopy dictates that quantitative or, at the very least, semi-quantitative data be obtained. The significance of these data is therefore dependent on knowing (1) the extent to which diffraction affects the spatial resolution and (2) the conditions needed to minimize diffraction.

Although diffraction theory can be employed to yield a qualitative relationship between wavelength, numerical aperture, and spectral interferences, a quantitative analysis requires the use of a more detailed theory or model experiments. In this investigation we report on model experiments which quantitatively assess the stray light produced in an infrared microscope. A comparison of single apertures, both before and after the sample, and dual apertures is made with regard to stray light effects. The effect of wavelength is also studied. Consequences of the findings will be discussed with regard to spatial resolution in the analysis of multilayer laminates and samples embedded in a host matrix. Diffraction theory will be used only in a qualitative sense to explain some of the important relationships and observations.

## EXPERIMENTAL

Infrared spectra were collected on a Spectra Tech IR-PLAN† microscope integrated with a Perkin-Elmer Model 1800 Fourier transform infrared spectrophotometer. The spectrophotometer uses a proprietary heated wire source operated at 1050°C, and a germanium-overcoated potassium bromide beamsplitter. Microscope optics included a 15× (N.A. = 0.58) objective, a 10× (N.A. = 0.71) condenser, and a liquid-nitrogen-cooled, narrow-band, mercury-cadmium-telluride (HgCdTe) detector. The detector was dedicated to the microscope and had an active area of 250 × 250 μm. Rectangular apertures were employed to isolate the samples and were fixed to the microscope to prevent alignment errors. Positioning of the sample was done manually in either bright-field or reflected light with the use of the existing illuminators. The entire optical path of the microscope was purged with nitrogen.

Double-sided interferograms were collected at 8 cm<sup>-1</sup> resolution with a mirror velocity of 1.5 cm/s. Two hundred fifty-six scans (two-minute data collect) were coadded for both the reference and sample. Interferograms were self-corrected for phase errors with the use of 128 points on either side of the centerburst. Transformation of these interferograms into spectra was performed with a fast Fourier transform and a medium Beer-Norton apodization function. All experimental results were obtained over a two-day period to minimize instrument instability. The signal-to-noise ratio (S/N) for the microscope system, determined after the experiments, was 4400 to 1 based on peak-to-peak noise. This value was determined with the use of a 100-μm pinhole as the sample and apertures both before and after this sample. Scan conditions for the S/N determination were as stated above.

The sample employed for this investigation was a free-standing film of cellulose acetate. The film was prepared by drawing an acetone solution of the material across a glass slide with the side of a glass pipette. Prior to application of the solution, a trough was formed on the glass slide by affixing Scotch‡ tape to both edges. After drying, the film could be cut to the desired dimension and peeled off the glass substrate. The film was mounted over a 6-mm-diameter circular opening in a black anodized aluminum slide. Positioning of the film was such that the film covered only half of the opening. Film thicknesses were controlled by adjusting the concentration of the solution to yield an infrared spectrum of the film in

Received 1 April 1991; revision received 14 June 1991.

\* Author to whom correspondence should be sent.

† IRPLAN is a registered trademark of Spectra Tech, Inc.

‡ Scotch brand tape is a registered trademark of 3M Corporation.

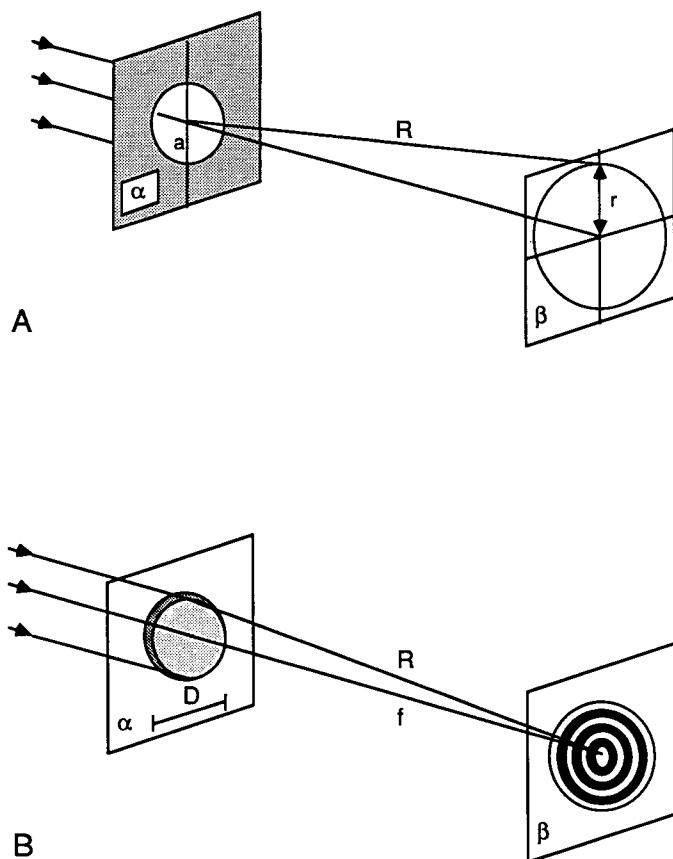


FIG. 1. (A and B) Diffraction at a circular aperture.

which the transmittance extremes were 100 and 20%. The same film sample was employed for the entire investigation, and its edge roughness did not exceed 0.5  $\mu\text{m}$ .

## RESULTS AND DISCUSSION

Under normal sampling conditions (i.e., samples whose sizes are twice the diffraction limit for the given system) the effects of diffraction are minimal. However, when spatial resolution and quantitative interpretation are pushed to the extremes, diffraction becomes a significant problem. Fresnel diffraction describes the interaction of light waves with various optical elements. A special case of Fresnel diffraction is Fraunhofer diffraction, which requires the light waves to be plane or collimated. By definition, the type of diffraction which occurs in the infrared microscope is Fresnel since the light is not exactly collimated. However, if the diffracting object is at a distance from the observation point which is much greater than the ratio of  $d^2/\lambda$ , where  $d$  is the diameter of the diffracting object and  $\lambda$  is the wavelength of light, the diffraction effects may be qualitatively expressed by the relationships describing Fraunhofer diffraction.<sup>1</sup>

Figure 1A illustrates plane waves passing through an aperture  $\alpha$  of radius  $a$ . The far field diffraction pattern observed on the screen  $\beta$  takes the form of the familiar Airy diffraction pattern illustrated in Fig. 1B. The central bright spot or maximum of this pattern is called the Airy disk. Its radius can be described in terms of the

physical dimensions of the aperture, the distance of the screen from the aperture, and the wavelength of light:<sup>2</sup>

$$r = \frac{1.22\lambda R}{2a}. \quad (1)$$

Here  $r$  is the radius of the Airy disk,  $a$  is the radius of the aperture,  $\lambda$  is the wavelength of light, and  $R$  is related to the distance between the screen  $\beta$  and the aperture. If a lens is placed in the aperture, as in Fig. 1B, the radius of the Airy disk can be described in terms of the physical characteristics of the lens:<sup>2</sup>

$$r = \frac{1.22\lambda f}{D} \quad (2)$$

for  $f$  approximately equal to  $R$ . Here  $f$  is the focal length of the lens, and  $D$  is the diameter of the lens. The more familiar form of the equation for high-magnification lenses relates the numerical aperture (N.A.) of the lens to the Airy disk as:

$$r = \frac{1.22\lambda}{2 \text{ N.A.}} \quad (3)$$

Diffraction and its effects can arise in an infrared microscope from many different sources. Several reports have been published showing the effects of diffraction produced by the sample, by improper aperturing, by wavelength, and by the central obscuration present in the reflecting objectives employed in the microscope.<sup>3-9</sup> The analyst has very little control over these sources, with the exception of the type of aperturing and, to a certain extent, the wavelength chosen for analysis. In some instances the sample can be manipulated (e.g., oblique microtoming) to yield enhanced separation of the layers.

Tracing a light ray through the optical train of the IRPLAN microscope illustrates that diffraction occurs at several optical components employed to isolate the sample of interest. Figure 2 shows the configuration of these optical components. First, the infrared source in the spectrometer is focused to a 3-mm-diameter image at the aperture before the sample. Diffraction of the source by this aperture occurs as a result of decreasing the aperture size to facilitate the analysis of samples smaller than 200  $\mu\text{m}$ . For example, if an 8- $\mu\text{m}$ -diameter sample is to be analyzed, the size of the aperture should be  $15\times$  larger, or 120  $\mu\text{m}$  (i.e., the aperture size is the product of the sample size and objective magnification). Since the aperture size required to analyze the 8- $\mu\text{m}$ -diameter sample is significantly smaller than the image of the source, diffraction will arise, as depicted in Fig. 1A. The light rays will further experience diffraction on being imaged from the aperture to the sample plane by the objective. If a point source is placed at the aperture instead of the extended infrared source image, the best and smallest diffraction-limited dimension obtainable at the sample plane is dictated by the N.A. of the objective and the wavelength of light in accordance with Eq. 3. For 9.5- $\mu\text{m}$ -wavelength light and an N.A. of 0.58, the diameter of the diffraction-limited image formed at the sample plane is 20  $\mu\text{m}$ . Once again, diffraction will spread light into an area larger than that of the sample for sample diameters of 20  $\mu\text{m}$  or less.

Similar diffraction occurs by imaging the sample

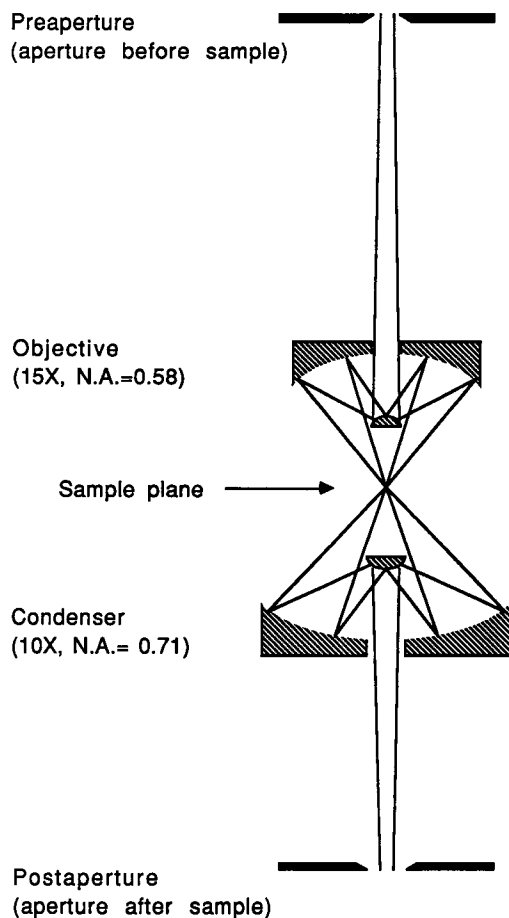


FIG. 2. Optical configuration of the IRPLAN microscope.

through the remaining elements of the optical train to the detector. For a self-luminous point sample imaged onto the aperture after the sample by the condenser, the best or smallest image formed at the aperture is determined by the product of the diffraction-limited dimension from Eq. 3 and the condenser magnification.<sup>1</sup> Thus, a  $163\text{-}\mu\text{m}$ -diameter image of the point source is formed at the aperture after the sample. From a consideration of the condenser magnification of  $10\times$ , analysis of an  $8\text{-}\mu\text{m}$ -diameter sample would dictate that the aperture after the sample be  $80\text{ }\mu\text{m}$  in diameter. Here again, the aperture is significantly smaller than the diffraction-limited diameter of the self-luminous point source. As a result, considerable diffraction will occur at the aperture.

As Messerschmidt points out,<sup>5</sup> the situation is somewhat worse for the following reasons: The relationship developed in the first few paragraphs describe the radius of the Airy disk. The Airy disk is defined as the central bright spot or light maximum and contains only 84% of the energy associated with the original source. The remaining energy is distributed in the lobes which occur at larger radii and, subsequently, areas outside that defined by the imaging elements. Second, the relationships are valid for an infinitely small point source or self-luminous sample being imaged through each of the optical components. In reality, the source and the sample have finite dimensions—which tends to broaden the Airy diffraction pattern still further.

From the above considerations it can be seen that the

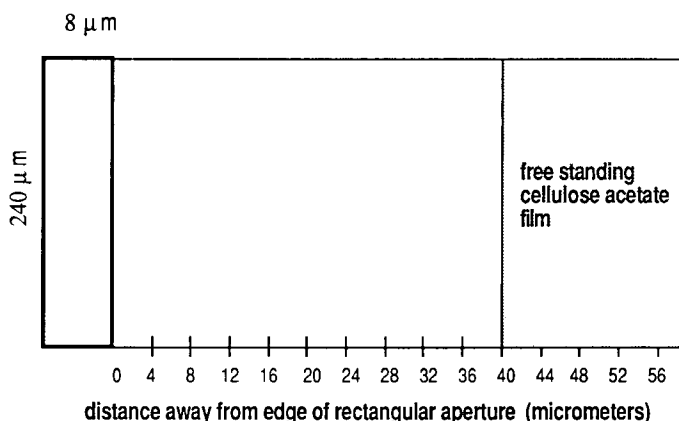


FIG. 3. Sample configuration employed to generate stray radiation profiles.

spatial profile of the source image or sample image is considerably altered on being imaged through the entire optical train of the microscope. By the time the image of the source reaches the sample it has undergone diffraction at the aperture, the objective, and the central obscuration of the objective. The image of the sample undergoes similar diffraction effects on being imaged through the optical train to the detector. As a result, the diffraction of the source and/or sample image through the microscope yields a spread function for the entire microscope which is the superposition of the diffraction patterns from each imaging element in the system. The spread function defines the extent to which a point source, imaged through an optical element, spreads outside its defined boundary.

Knowing the spread function of the individual optical components in the infrared microscope is not important from the analyst's standpoint since most, if not all, elements are employed during a measurement. Knowing the spread function for the entire microscope system under different conditions is important because it will allow the true spatial resolution of the system to be determined. Figure 3 schematically illustrates the method by which radiation falling outside the sample area defined by the system was determined. In an initial experiment, an  $8 \times 240\text{ }\mu\text{m}$  aperture placed between the source and the sample was used to collect a background spectrum. The left-most edge of the free-standing cellulose acetate film was then stepped away from the right-most edge of the aperture image, and transmission spectra were collected at each position. Theoretically, if no diffracted light is present outside the area defined by the aperture, a true 100% transmittance line should be observed. Figure 4 shows a reference infrared spectrum of the cellulose acetate film recorded within the  $8 \times 240\text{ }\mu\text{m}$  aperture. Figure 4 also illustrates spectra of the same film but with its edge located next to and  $40\text{ }\mu\text{m}$  away from the edge of the aperture image, respectively. These latter two spectra clearly demonstrate that diffracted radiation is present in areas outside that defined by the aperture. Perhaps the most surprising result is that absorptions attributed to the cellulose acetate film can be observed when the edge of the film is  $40\text{ }\mu\text{m}$  away from the edge of the aperture image. The spectra also show that this stray radiation has larger components at longer

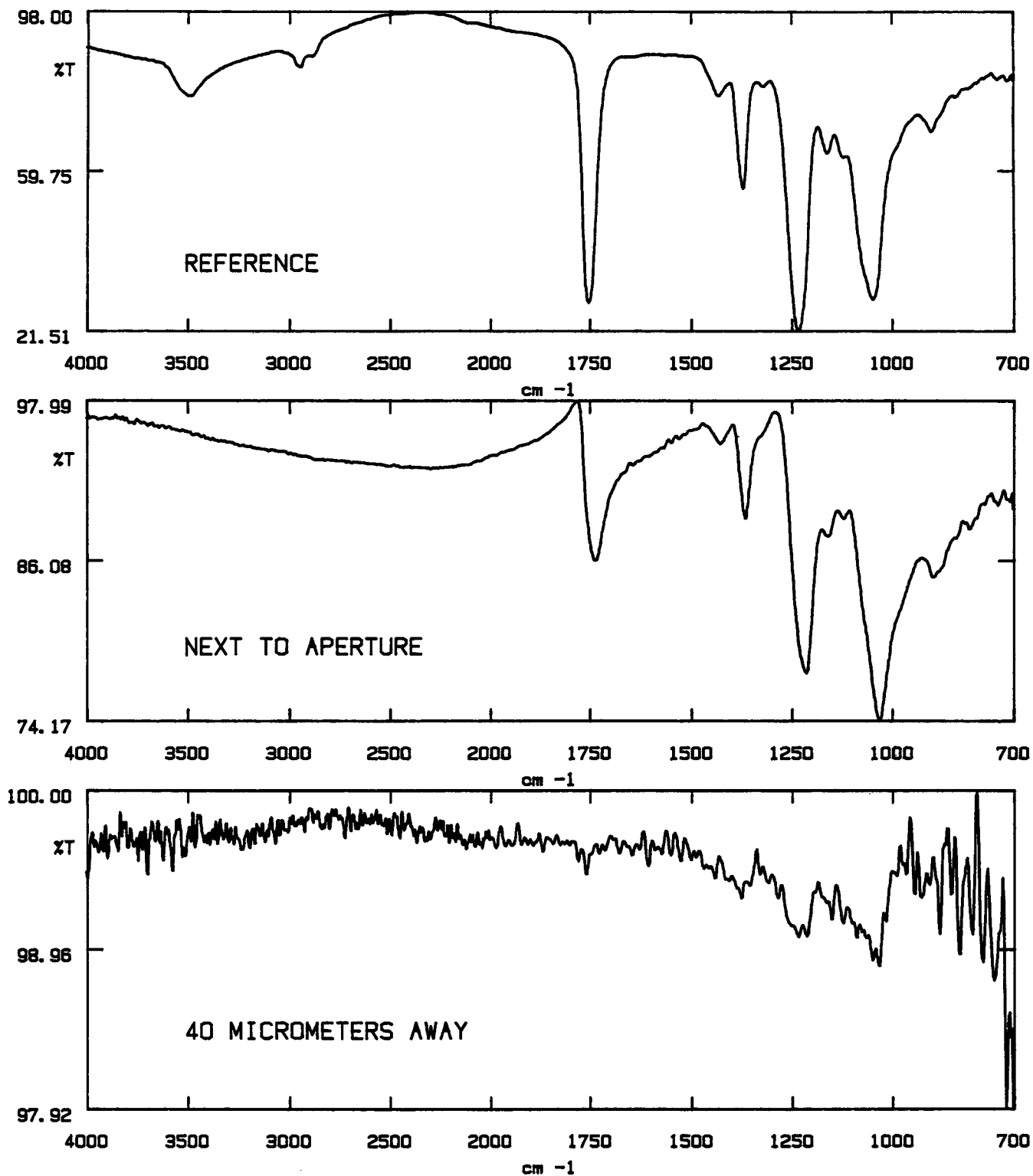


FIG. 4. Spectra of cellulose acetate film obtained with  $8 \times 240 \mu\text{m}$  apertures before the sample. (Top) reference; (middle) film edge aligned with edge of aperture image; (bottom) film edge aligned  $40 \mu\text{m}$  away from edge of aperture image.

wavelengths. A comparison of the intensity of the C-O-C asymmetric stretch to that of the C=O stretch in each spectrum shows that the intensity of the C-O-C stretch is much stronger in the spectra obtained outside the area defined by the aperture. This simple example clearly shows that, if steps are not taken to determine the extent of diffraction, the results of a mapping type analysis will

not be very reliable unless the individual layers of a cross-sectioned laminate are nearly  $100 \mu\text{m}$  thick or larger. The same criterion holds true for an isolated particle embedded in a surrounding matrix. This latter situation is even more severe since the sample geometry is such that diffraction is occurring in two dimensions. In the present investigation the aperture dimension corresponding to

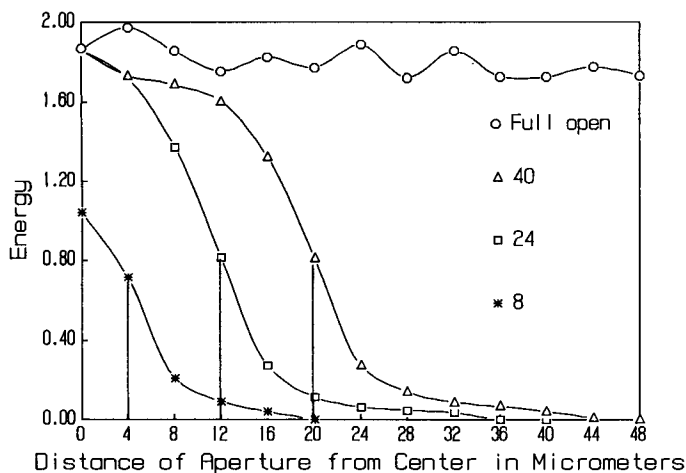


FIG. 5. Source profiles formed at the sample plane for various aperture sizes (aperture placed before sample).

the y-axis was purposely made much larger than the x-dimension so that diffraction in the x-dimension would dominate. This configuration is also consistent with those employed for the analysis of multilayer laminates.

A second experiment was conducted to determine the profile of the source image formed at the sample plane when various aperture sizes before the sample were employed. In this experiment no polymer film was used. The profiles were obtained by setting the aperture before the sample to the desired size and centering this aperture in the field of view. The aperture after the sample was then set to a size of  $8 \times 240 \mu\text{m}$  and used to analyze discrete ( $8\text{-}\mu\text{m}$ ) sections of the source image at the sample plane. These measurements were done by maintaining the aperture before the sample at a fixed position and translating the  $8 \times 240 \mu\text{m}$  aperture after the sample away from the center of the field of view in  $4\text{-}\mu\text{m}$  steps. Figure 5 shows the results of these experiments, which are plotted as a function of energy and distance of the aperture after the sample away from the center of the field of view.

Aperture settings before the sample of 8, 24, and  $40 \mu\text{m}$  represent sample diameters which are below, slightly larger than, and above the diffraction-limited dimensions, respectively. The diffraction-limited dimensions are dictated by Eq. 3 with an objective N.A. = 0.58 and a wavelength of  $9.5 \mu\text{m}$ . Ideally, the source profile formed at the sample plane for the various aperture settings should be an edge or step function. The general shape of the curves indicates that aperture dimensions above the diffraction limit (e.g.,  $40 \mu\text{m}$ ) more closely approximate an edge function, as described by Messerschmidt.<sup>6</sup> At dimensions below the diffraction limit, the image profile takes on the shape of the Airy pattern. At the diffraction limit, the profile is somewhat intermediate between an edge function and the Airy pattern. The vertical lines drawn for each curve in Fig. 5 delineate the position (i.e., the image of the aperture edge) at which the energy should drop to zero, assuming an ideal edge function. As a result of diffraction, stray energy extends past this edge and illuminates those areas not defined by the aperture. The problem is most severe for the  $8\text{-}\mu\text{m}$  aperture setting, which demonstrates that a larger percentage of energy

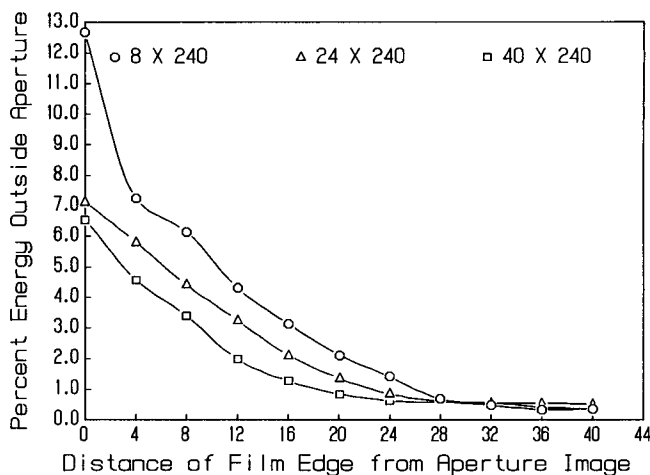


FIG. 6. Percent of stray energy outside area defined by aperture for various aperture sizes (apertures placed before and after sample).

is redistributed to areas not defined by the aperture. On comparison, as the aperture dimension is increased, the percentage of stray energy present outside the edge of the aperture image is reduced. Figure 5 also illustrates the profile of the imaged source when the aperture before the sample is completely open. The fluctuations, or ringing, in this profile at different locations are normal for diffraction at a high contrast edge.<sup>10</sup>

In order to quantitatively assess the stray energy present past the edge of the aperture image, the initial experiment employing the polymer film was conducted with the use of different aperture sizes and aperturing modes. As a further illustration of the significance of these experiments in terms a spectroscopist can easily digest, the integrated intensity of the C-O-C absorption ( $9.5 \mu\text{m}$ ,  $1050 \text{ cm}^{-1}$ ) in those spectra obtained outside the aperture was ratioed to that of the reference spectrum obtained within the aperture. This ratio was then plotted as a function of the distance of the film edge from that of the aperture image. The ratios are the average of three different measurements taken at each position. The uncertainty in the ratios does not exceed 0.5%.

Figure 6 illustrates the data collected for three different aperture dimensions with apertures both before and after the sample. The curves clearly demonstrate that the amount of stray radiation, present outside the area defined by the apertures, becomes larger as the dimension of the apertures decreases. Again the surprising result is that noticeable (i.e., 1–2%) stray radiation is present when the film edge is  $24 \mu\text{m}$  away from the edge of the aperture image. A common practice in infrared microspectroscopy is to over-aperture the sample to ensure that spectral impurities from neighboring samples are minimized. These data demonstrate that, for small samples (samples less than  $40 \mu\text{m}$  in diameter), over-aperturing will actually increase spectral impurities from neighboring samples.

Figure 7 illustrates the percent of diffracted light present outside the areas defined for apertures ( $8 \times 240 \mu\text{m}$ ) placed before the sample, after the sample, and both before and after the sample. The results demonstrate that a significant amount of stray light is present when only the aperture after the sample is employed. At 36

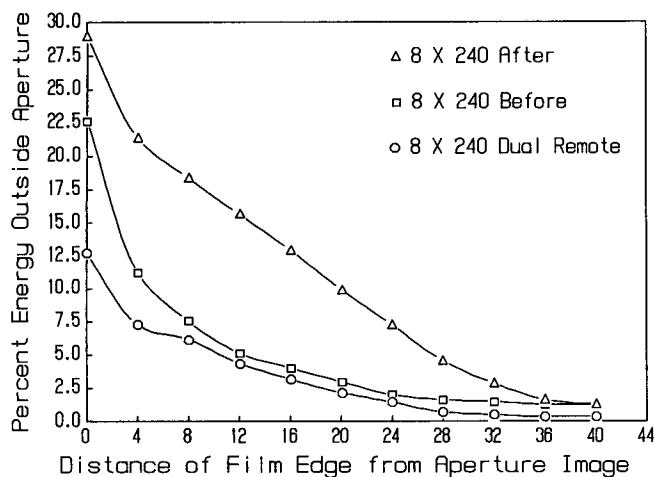


FIG. 7. Percent of stray energy outside area defined by aperture for various aperturing modes ( $8 \times 240 \mu\text{m}$  aperture size).

$\mu\text{m}$  away from the edge of the aperture image, more than 2% of stray radiation is detected. Employing only the aperture before the sample reduces the amount of stray light reaching the detector. This reduction is such that 2% is observed at only  $24 \mu\text{m}$  away from the aperture, and at  $32 \mu\text{m}$  away from the aperture the amount of impure or stray radiation has dropped to well below 1%. Employing apertures both before and after the sample reduces the stray light still further. In this case an equal amount of stray light is observed only out to  $20 \mu\text{m}$  away from the edge of the aperture. If an acceptable level of stray light is 2%, then the spatial resolutions for aperturing after, before, and before and after the sample are 72, 48, and  $40 \mu\text{m}$ , respectively.

An explanation for the vast difference in stray light observed when aperturing after the sample as opposed to before the sample arises from the fact that the aperture before the sample limits the source image to illuminate only the sample of interest. An idealized depiction of the source image formed at the sample plane for both aperturing modes is shown in Fig. 8. Under the best conditions, the image of the source formed at the sample or sample plane has an Airy disk whose diameter is approximately  $20 \mu\text{m}$ . This dimension is also very close to that which was measured experimentally for the source profile (Fig. 5, profile for  $8\text{-}\mu\text{m}$  aperture). Figure 8A shows the Airy diffraction pattern of the source superimposed on the sample of interest or, in the present experimental case, the area which should be defined by the aperture (i.e.,  $8 \times 240 \mu\text{m}$ ). The outside arrows delineate the extent of the Airy disk. As a result of diffraction, energy is spread into areas not defined by the aperture. Thus, if the edge of the polymer film is aligned with the edge of the aperture image, absorptions of the film will still be observed as a result of the diffracted light. The percent of stray radiation will decay in accordance with the Airy profile on stepping the film edge out to greater distances from the edge of the aperture image.

Figure 8B illustrates the case for aperturing after the sample. Since no aperture is present before the sample, the sample is illuminated by an entire image of the source. In the IRPLAN, the image of the source at the sample plane is  $200 \mu\text{m}$  in diameter. Due to diffraction, the in-

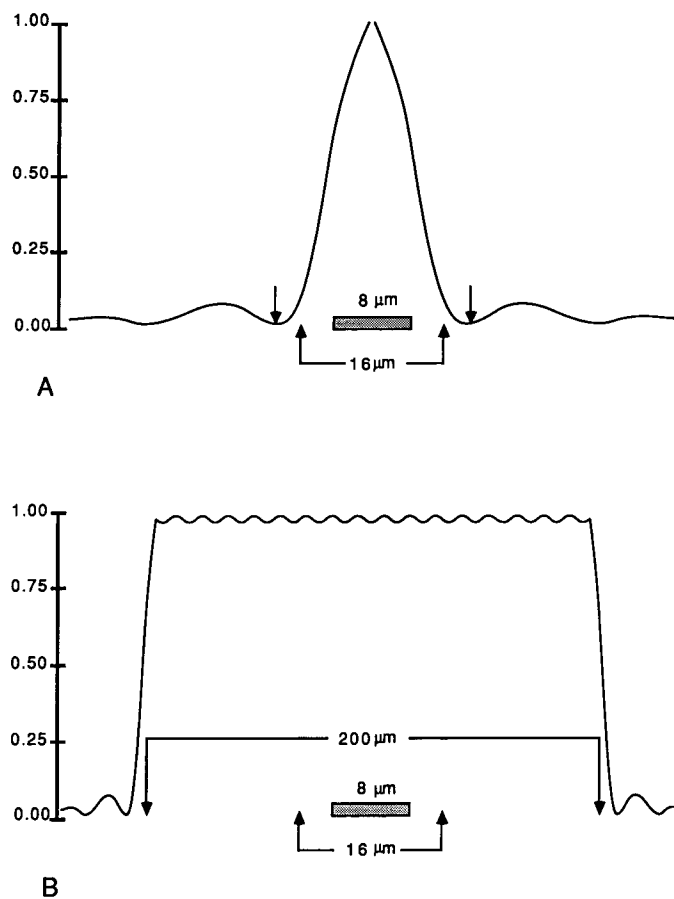


FIG. 8. Idealized source energy distributions formed at the sample plane for aperturing before the sample (A) and after the sample (B).

tensity distribution will not be a perfect edge function but one whose intensity distribution is as shown in the figure. In this aperturing mode, the spatial resolution or ability to observe the image of one sample without interferences from a neighboring sample is again dictated by Eq. 3. Thus the element forming the image of the sample at the aperture after the sample can do so with a spatial resolution of  $16 \mu\text{m}$  (based on  $\text{N.A.} = 0.71$ ). In other words, under the best conditions, the diameter of the smallest sample that one can observe with this element while maintaining spectral purity is  $16 \mu\text{m}$ .

As a result of diffraction, the area viewed by the optical element is larger than that defined by the aperture. Placing the edge of a polymer film next to the edge of the aperture image at the sample plane will result in absorptions being observed from the stray radiation present in these areas. Here again the stray radiation will follow the profile of the intensity distribution on stepping the film edge to larger distances from the aperture edge. In contrast, the intensity will not decay, as in the case of the Airy profile, but will remain relatively constant, thereby yielding higher stray energy for this aperturing mode.

Finally, Fig. 9 demonstrates the effect of diffraction in terms of wavelength. This figure compares the percent of stray radiation present outside the area defined by the aperture for both the C-O-C asymmetric stretch ( $9.5\text{-}\mu\text{m}$ -wavelength light) and the C=O stretch ( $5.72\text{-}\mu\text{m}$ -wavelength light). Apertures both before and after the

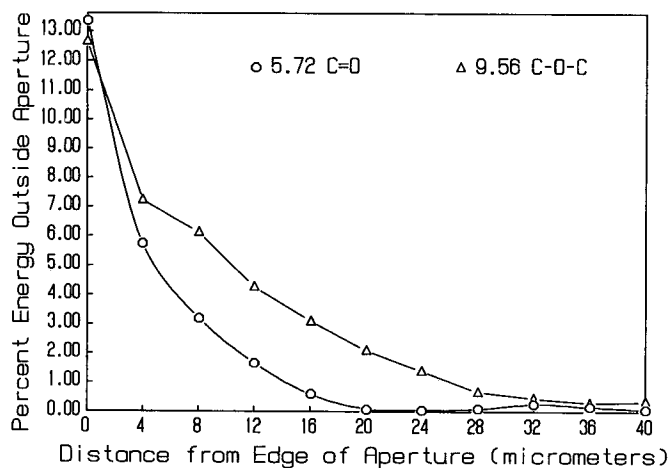


FIG. 9. Percent of stray energy outside area defined by aperture for different wavelengths (apertures placed before and after sample).

sample with dimensions of  $8 \times 240 \mu\text{m}$  were employed. The figure illustrates, in accordance with relationships 1-3, that diffraction is more severe for longer wavelengths. By choosing the carbonyl absorption as the analytical peak, one can effectively reduce the stray light. On the basis of an acceptable stray light level of 1%, the spatial resolution with the use of the C-O-C absorption is  $56 \mu\text{m}$ , whereas that for the carbonyl absorption is only  $32 \mu\text{m}$ . The implication for quantitative analysis is that, if mapping analysis is done on the basis of functional groups, those groups with absorptions occurring at shorter wavelengths should be employed to maximize the spatial resolution and thus the quantitative integrity of the data collected.

The emphasis in this investigation was placed on the study of those variables related to diffraction which can be controlled by the analyst (i.e., aperturing mode, aperture size, and choice of analytical wavelength). Although it has been shown that diffraction occurs from the use of Cassegrainian condensers and objectives, the analyst has no control over these design parameters. It should be stated that the experiments conducted employed the use of a model sample under ideal conditions. A thin free-standing film was chosen to minimize errors such as diffraction from the sample and changes in image planes associated with differing refractive indices of a supporting substrate. Under conditions where normal nonideal laminates are studied, it is expected that these errors will introduce stray light errors into the analysis. In addition to these errors a laminate presents a sample configuration in which waveguiding of the infrared light through the individual layers could have a dramatic effect on the pathlength of the light through the sample and quite possibly the spatial resolution. Here again mapping analyses which infer some level of quantitation with regard to spatial resolution will require a careful characterization of the sample and system variables.

While some of the results may be helpful for improving future microscope designs, they are only valid for a design similar to the IRPLAN. Those microscopes which employ off-axis elements to image the infrared source onto the sample will exhibit different stray light characteristics. It is expected that the stray light will be more problematic in microscopes of this design since the off-

axis elements are not diffraction limited in terms of imaging, and the aperturing, because of a design constraint, is done after the sample. This expectation is not to say that mapping analyses cannot be conducted with these microscopes but that the quantitative integrity of the data will be limited or compromised.

## CONCLUSIONS

The results of the investigation have shown that the apertures which are employed to spatially isolate the sample of interest are responsible for most of the diffraction occurring in an infrared microscope. In general, the extent of diffraction (spread function analysis) for different aperturing modes can be described by the Airy function provided that the aperture dimension is below that dictated by diffraction. For aperture dimensions far above the limit, an edge function is sufficient to describe the energy distribution. Aperture dimensions at or just above the diffraction limit are described as intermediate between the Airy and edge functions. As predicted by the diffraction relationships, decreasing the size of the aperture will increase the amount of stray energy present in those areas not defined by the geometrical image of the aperture. In this view the common practice of over-aperturing will work only for relatively large samples. As the sample size approaches the diffraction limit, over-aperturing will actually increase spectral impurities from neighboring samples.

The results have also shown that spatial resolution estimates based of the relationships developed for the Airy disk (central maximum of the Airy pattern) are insufficient if quantitative analysis is to be attempted. The diameter of the Airy disk for the present experimental conditions is  $20 \mu\text{m}$ . If a stray light level of only 1% can be tolerated, the experimental results show that the spatial resolution is at best  $56 \mu\text{m}$  when an aperture of  $8 \mu\text{m}$  is employed. As a result, the spatial resolution determined from the relationships is underestimated by a factor of three.

The mode of aperturing will also have significant consequences with regard to the quantitative integrity of the data collected in a mapping analysis. The results have shown with the current microscope configuration that apertures employed both before and after the sample provide the best means to reduce the amount of stray light for a given measurement. If only one aperture is to be employed, best results are obtained with the aperture before the sample.

Finally, the judicious choice of analytical wavelength or absorption for a mapping analysis will also reduce the amount of stray light present in a given measurement. This observation is again consistent with the diffraction relationships.

1. M. Pluta, *Advanced Light Microscopy* (Elsevier, Amsterdam, 1988), Vol. 1.
2. E. Hecht and A. Zajac, *Optics* (Addison-Wesley Publishing Co., Reading, Massachusetts, 1974).
3. P. H. Turner, *Anal. Proc.* **23**, 268 (1986).
4. D. B. Chase, "Infrared Microscopy: A Single Fiber Technique," in *The Design, Sample Handling, and Applications of Infrared Microscopes*, ASTM STP 949, P. B. Roush, Ed. (ASTM, Philadelphia, 1987), pp. 4-11.

5. R. G. Messerschmidt, "Photometric Considerations in the Design and Use of Infrared Microscope Accessories," in *The Design, Sampling Handling and Applications of Infrared Microscopes*, ASTM STP 949, P. B. Roush, Ed. (ASTM, Philadelphia, 1987), pp. 12–26.
6. R. G. Messerschmidt, "Minimizing Optical Nonlinearities in Infrared Microspectrometry," in *Infrared Microspectroscopy; Theory and Applications*, R. G. Messerschmidt and M. A. Harthcock, Eds. (Marcel Dekker, New York, 1988), pp. 1–19.
7. A. J. Sommer and J. E. Katon, in *Microbeam Analysis*, Dale E. Newbury, Ed. (San Francisco Press, San Francisco, California, 1988), pp. 207–214.
8. P. L. Lang, A. J. Sommer, and J. E. Katon, "Infrared and Raman Microspectroscopy: An Overview of Their Use in the Identification of Microscopic Particulates," in *Particles on Surfaces II*, K. L. Mittal, Ed. (Plenum Publishing, New York, 1989), pp. 143–161.
9. J. E. Katon, A. J. Sommer, and P. L. Lang, *Appl. Spectrosc. Rev.* **25**, No. 3 & 4, 173 (1989–1990).
10. M. Born and E. Wolf, *Principles of Optics* (Pergamon Press, London, 1965), 3rd ed.